Edge Detection of Magnetic Sources Using Enhanced Total Horizontal Derivative of the Tilt Angle

Geliştirilmiş Eğim Açısı Toplam Yatay Türevi ile Manyetik Kaynakların Sınırlarının Belirlenmesi

MUZAFFER ÖZGÜ ARISOY[1]*, ÜNAL DİKMEN[2]

[1]Cumhuriyet Üniversitesi, Mühendislik Fakültesi, Jeofizik Mühendisliği Bölümü, Merkez Kampüs, Sivas

[2]Ankara Üniversitesi, Mühendislik Fakültesi, Jeofizik Mühendisliği Bölümü, 06100 Tandoğan, Ankara

ABSTRACT

This study suggests a new edge-detection filter, called enhanced total horizontal derivative of the tilt angle (ETHDR). ETHDR is the total horizontal derivative of the ratio of the vertical derivative to the total horizontal derivative of the first order analytical signal amplitude. This paper compares the results of ETHDR and other normalized derivative filters. The feasibility and capability of the ETHDR method is demonstrated using a theoretical data and a real magnetic dataset. Compared with the other derivative based filters, the ETHDR produces more detailed results for deeper magnetized structures and gives sharp response over edges of sources.

Anahtar Kelimeler: Edge detection, imaging, magnetic anomalies

ÖZ

Bu çalışmada, geliştirilmiş eğim açısı toplam yatay türevi (ETHDR) olarak anılan yeni bir kenar belirleme süzgeci önerilmiştir. ETHDR düşey türevin analitik sinyal genliğinin toplam yatay türevine oranının toplam yatay türevi olarak verilmektedir. Bu çalışmada, ETHDR yöntemi ile diğer türev tabanlı süzgeçlerin sonuçları karşılaştırılmıştır. ETHDR yönteminin uygulanabilirlik ve yetenekleri sentetik ve gerçek arazi verisi üzerinde sınanmıştır. Diğer türev tabanlı süzgeçlerle karşılaştırıldığı zaman ETHDR yönteminin derin mıknatıslanmış yapılar için daha detaylı sonuçlar ürettiği ve kaynak yapılar üzerinde keskin bir cevap verdiği görülmüştür.

Keywords: Kenar belirleme, görüntüleme, manyetik belirtiler

M. Arısoy
e-posta: arisoy@cumhuriyet.edu.tr

INTRODUCTION

Delineating edges of magnetized structures is a common application of magnetic data to geological interpretation. Horizontal and vertical derivatives are routinely used to enhance details in magnetic data. The total horizontal derivative and analytical signal are two effective tools that are used to detect the edges of magnetized structures (Pilkington and Keating, 2004; Cooper and Cowan, 2008; Cooper, 2009). However, if the dataset contains features with a large variation in amplitude, then the features with small amplitudes may be difficult to outline.

In recent years, a number of methods, called balanced or normalized derivative methods, were introduced to overcome this problem (Cooper and Cowan, 2006). As a result of the exponential increase in computing power and the widespread use of geophysical commercial software packages, these methods are being used more effectively.

EDGE DETECTION

A commonly used edge detection filter is the total horizontal derivative (THDR) and is given by (Cordell and Grauch, 1985) as:

$$THDR = \sqrt{\left(\frac{\partial T}{\partial x}\right)^2 + \left(\frac{\partial T}{\partial y}\right)^2} \qquad (1)$$

where T is the magnetic field, $\partial T/\partial x$ and $\partial T/\partial y$ are the two orthogonal horizontal derivatives of the magnetic field. Figure 1a shows the magnetic response of three vertical-sided prisms with depths to the top of 1, 3 and 5 km from northwest corner to south-east corner, respectively. Uniformly distributed random noise of amplitude equal to 0.5% of the maximum magnetic data amplitude is added to the magnetic data. In terms of similarity, the magnetization intensity of all bodies is set at 1 A/m, and all bodies have a 5km depth extent. It is clear that all magnetized bodies produce a visible anomaly (Figure 1a), but the edges of the third body in the southeast region, the deepest, are difficult to delineate. Figure 1b shows the THDR of magnetic anomaly in Figure 1a. Imaging edges

of the deeper prism is poor while edges of the shallower bodies are well mapped. Thus, one can concluded that THDR is more effective in imaging shallower bodies than deeper one.

The expression of the amplitude of the analytical signal (AS) for 3D structures is given by Roest et al (1992) as:

$$AS = \sqrt{\left(\frac{\partial T}{\partial x}\right)^2 + \left(\frac{\partial T}{\partial y}\right)^2 + \left(\frac{\partial T}{\partial z}\right)^2} \qquad (2)$$

where $\partial T/\partial z$ is the vertical derivative of the magnetic field. The maxima of AS is very useful for delineating edges of magnetic sources because of the amplitude of the analytical signal peaks over magnetic sources. The most important benefit of the analytical signal is that, in the 2D case, it is independent of the magnetization direction, but this is not true in the 3D case (Li, 2006). However, if more than one magnetic source is present, the result of the analytical signal is dominated by shallow sources. Figure 1c shows an AS map of the magnetic data in Figure 1a. The maxima of AS of the magnetic data produce clear resolution of the shallower bodies, but do not delineate the deeper body very well.

A number of methods have been proposed to make subtle anomalies more visible. The first filter developed for this purpose was the tilt angle (Miller and Singh, 1994), which is the ratio of the vertical derivative to the absolute value of the horizontal derivative of the magnetic field:

$$Tilt = \tan^{-1}\left(\frac{\frac{\partial T}{\partial z}}{THDR}\right) \qquad (3)$$

The tilt angle amplitudes are restricted to values between $-\pi/2$ and $+\pi/2$; thus the method delimitates the amplitude variations into a certain range. Tilt angle therefore functions like an automatic-gain-control filter, and therefore responds equally well to shallow and deep sources. The amplitude of the tilt angle is positive over the magnetic sources, crosses through zero at or near the edge of the source, and is negative outside the source. Figure 1d shows the tilt angle of the magnetic data in Figure 1a.
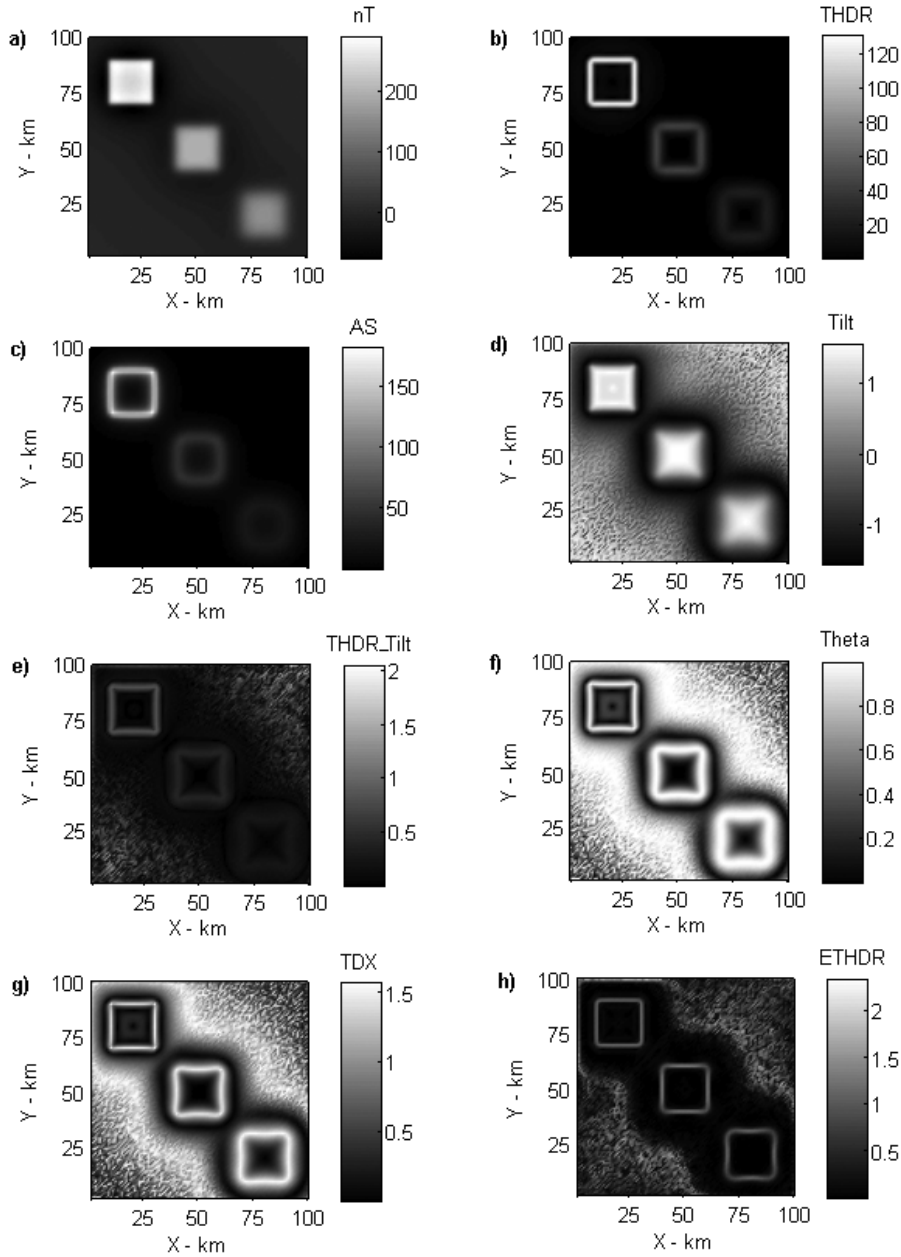
Figure 1. A comparison of derivative-based filters: (a) Synthetic magnetic data resulted from three prismatic bodies with depths of 1, 3 and 5 km from north-west corner to south-east corner, respectively. Image covers 100×100 km area. Uniformly distributed random noise of amplitude equal to 0.5% of the maximum magnetic data amplitude is added to the magnetic data. (b) Total horizontal derivative of magnetic data in (a). (c) Analytical signal of magnetic data in (a). (d) Tilt angle of magnetic data in (a). (e) Total horizontal derivative of the tilt angle (THDR_Tilt) of magnetic data in (a). (f) Theta map of magnetic data in (a). (g) Horizontal tilt angle (TDX) of magnetic data in (a). (h) Enhanced total horizontal derivative of the tilt angle (ETHDR) of magnetic data in (a).

Şekil 1. Türev tabanlı süzgeçlerin karşılaştırılması: (a) Kuzey-batıdan güney doğuya doğru sırasıyla derinlikleri 1, 3 ve 5 km olan üç prizmatik yapıdan hesaplanan yapay manyetik veri. Görüntü 100×100 km' lik bir alanı göstermektedir. Manyetik veriye, manyetik verinin en büyük genlik değerinin 0.5%' i kadar gelişigüzel rastsal gürültü eklenmiştir. (b) (a)' da verilen manyetik verinin toplam yatay türevi. (c) (a)' da verilen manyetik verinin analitik sinyali. (d) (a)' da verilen manyetik verinin eğim açısı. (e) (a)' da verilen manyetik verinin eğim açısı toplam yatay türevi (THDR_Tilt). (f) (a)' da verilen manyetik verinin Theta haritası. (g) (a)' da verilen manyetik verinin yatay eğim açısı (TDX). (h) (a)' da verilen manyetik verinin geliştirilmiş eğim açısı toplam yatay türevi (ETHDR).

The tilt angle is relatively smooth and positive over the bodies. It can be followed that the response of the tilt angle is blurred due to the model depth. The tilt angle produces a zero value over the source edges.

Verduzco et al (2004) presented an edge detector, which is the total horizontal derivative of the tilt angle (THDR_Tilt):

$$THDR\_Tilt = \sqrt{\left(\frac{\partial Tilt}{\partial x}\right)^2 + \left(\frac{\partial Tilt}{\partial y}\right)^2} \qquad (4)$$

THDR_Tilt is independent of the geomagnetic field and generates maximum values over the edges of the magnetized bodies. Figure 1e shows the THDR_Tilt of the magnetic data in Figure 1a. The THDR_Tilt delineates model edges well, as the amplitude of the THDR_Tilt peaks over magnetic sources, but the results for the deeper bodies are not so effective. Moreover, in the presence of noise, the THDR_Tilt strongly amplifies noise in the data (Figure 1e).

Wijns et al (2005) introduced the Theta map (θ), which is the normalization of the THDR by the AS:

$$\cos\theta = \left(\frac{THDR}{AS}\right) \qquad (5)$$

Figure 1f shows the theta map of the magnetic data in Figure 1a. The theta map delineates model edges well, but the response of deeper bodies is diffused; consequently, it does not produce the expected sharp gradient over the edges.

Recently, Cooper and Cowan (2006) presented the horizontal tilt angle method (TDX) as an edge detector:

$$TDX = \tan^{-1}\left(\frac{THDR}{\left|\frac{\partial T}{\partial z}\right|}\right) \qquad (6)$$

The horizontal tilt angle is the normalization of the amplitude of the total horizontal derivative by the vertical derivative. Figure 1g shows the TDX of the magnetic data in Figure 1a. TDX responds equally well to shallow and deep bodies, and also delineates the edges of all the bodies well. TDX has a much sharper gradient over the edges of the magnetized bodies. The geometric illustrations of the THDR, AS, Tilt and TDX are shown in Figure 2.

EDGE ENHANCEMENT USING THE ENHANCED TOTAL HORIZONTAL GRADIENT OF THE TILT ANGLE

The use of THDR and AS filters in magnetic data interpretation is traditional. However, when the data contain magnetic anomalies with a wide range of amplitudes, the results of THDR and AS filters are frequently dominated by high-amplitude anomalies, obscuring subtle anomalies. Balanced or normalized derivative methods have been introduced to overcome this problem. However, the results of the normalized derivative methods for the deeper bodies are not so effective, as response is blurred due to the source depth. In this study a new edge detector is introduced to overcome this problem.

The proposed ETilt filter is the ratio of the vertical derivative to the total horizontal derivative of the AS:

$$ETilt = \tan^{-1}\left(k\frac{\frac{\partial T}{\partial z}}{\sqrt{\left(\frac{\partial A}{\partial x}\right)^2 + \left(\frac{\partial A}{\partial y}\right)^2}}\right) \qquad (7)$$

where

$$k = \frac{1}{\sqrt{dx^2 + dy^2}} \qquad (8)$$

k is the dimensional correction factor. *dx* and *dy* are sampling intervals in the *x* and *y* directions, respectively. The dimensional correction factor, k, does not have an effect on the Etilt response. We suggest the use of the total
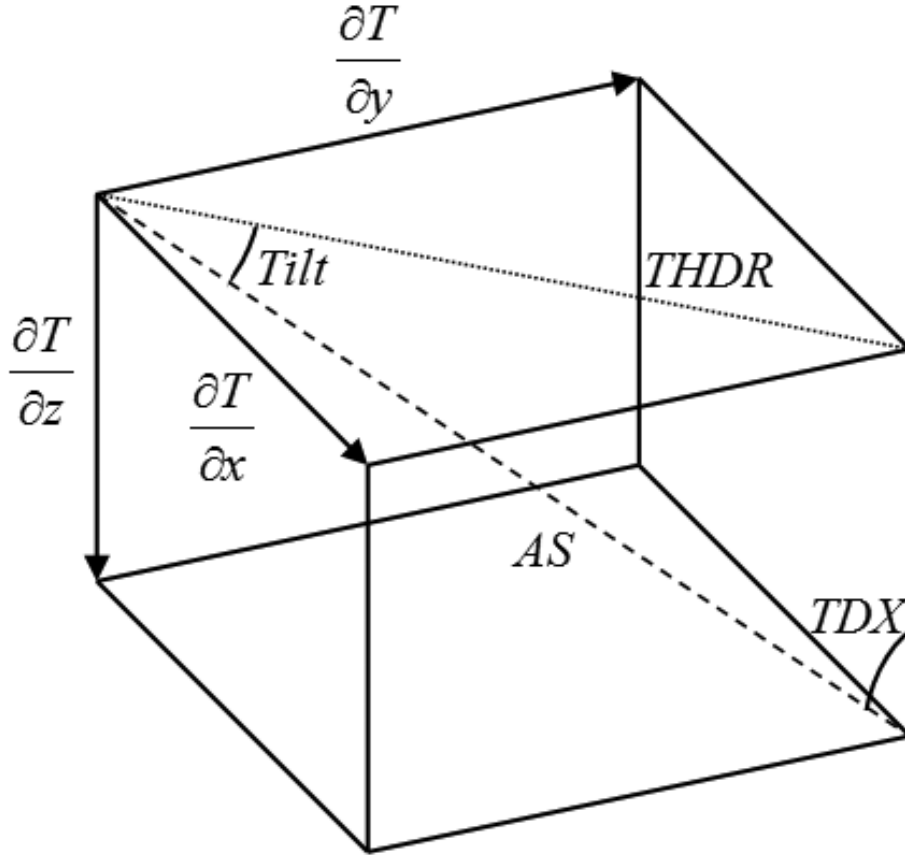
Figure 2. The geometric definitions of the THDR, AS, Tilt and TDX.
Şekil 2. THDR, AS, Tilt ve TDX' nın geometrik anlamları.

horizontal derivative of the ETilt as an edge detector (enhanced total horizontal derivative of the tilt angle-ETHDR):

$$ETHDR = \sqrt{\left(\frac{\partial ETilt}{\partial x}\right)^2 + \left(\frac{\partial ETilt}{\partial y}\right)^2} \qquad (9)$$

Figure 1h shows the ETHDR of the magnetic data in Figure 1a. The ETHDR delineates the edges of the all bodies better than the filters discussed above, as it produces a very sharp gradient over the edges of the bodies. Thus, structural interpretation is very easy and powerful using the presented method. Most normalized derivative methods are so effective not only shallow bodies but also deeper bodies (see Figure 1d-g), but all normalized derivative methods present a diffuse response to deeper structures. However, the presented method produces very clear resolution, not only in shallow bodies but also deeper bodies. Thus, if more than one magnetic source is present, and some of the sources are very close to each other, the ETHDR filter outlines the edges of bodies very well. The responses of existing filters, ETilt and ETHDR filters to 2D prism and vertical contact models are given in Figure 3. Figure 3 gives readers a much better idea of the behavior of the ETHDR method. The ETHDR peaks over the edges of the model and the distance of the drop to half of the peak amplitude is very narrow, as expected from an edge detector (see Figure 3). The method is dependent of geomagnetic inclination. For this reason, the data should be previously reduced to pole. A disadvantage of the presented method is that, because the ETHDR filter uses derivatives of a derivative-based filter, it strongly amplifies noise
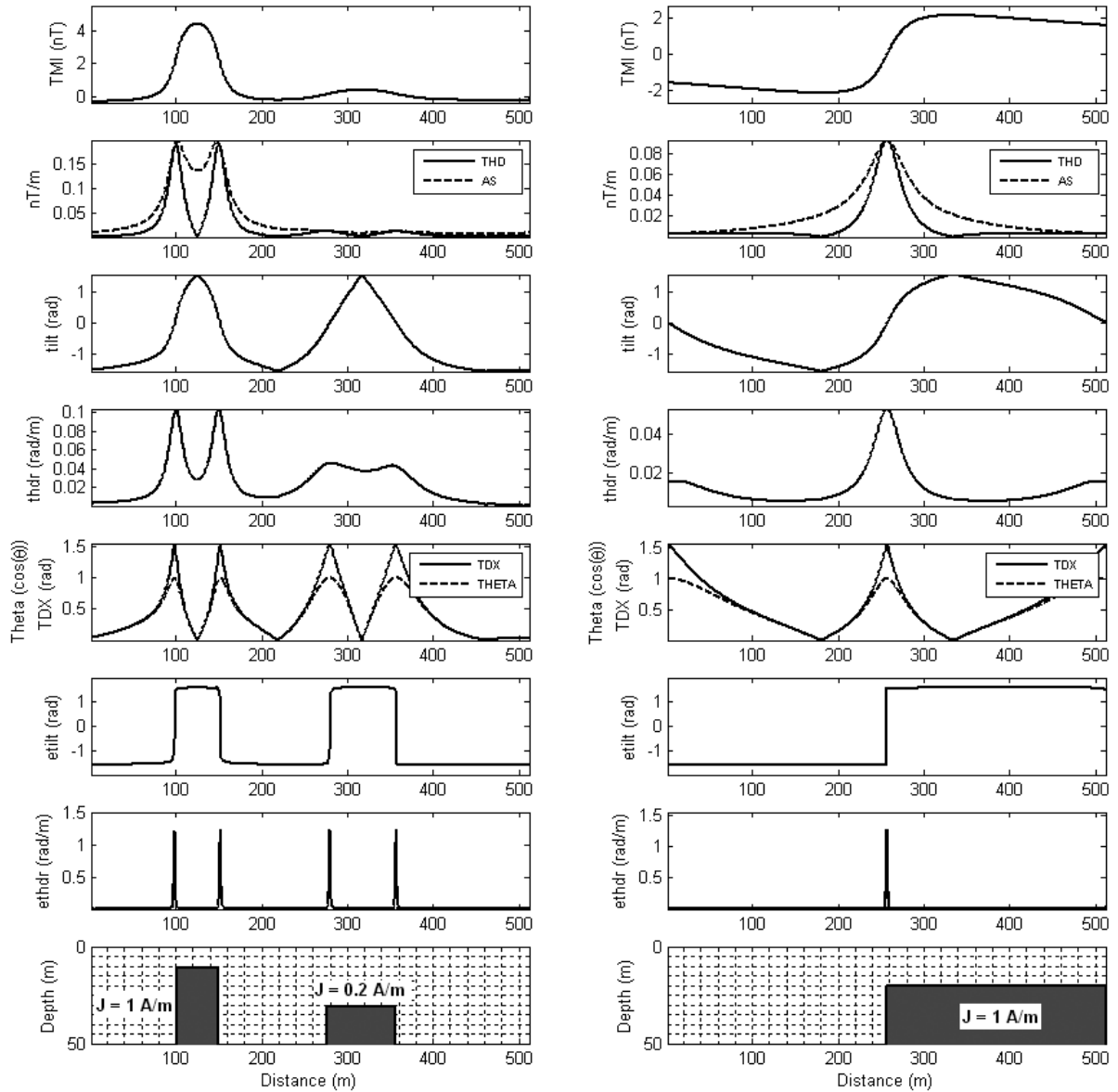
Figure 3. Magnetic, THDR, AS, Tilt, THDR_Tilt, Theta, TDX, ETilt and ETHDR responses resulted from 2D prism and vertical contact models. All bodies are magnetized in a vertical field.

Şekil 3.   2B prizma ve düşey kontak modellerinin manyetik, THDR, AS, Tilt, THDR_Tilt, Theta, TDX, ETilt ve ETHDR cevapları. Tüm yapılar düşey alanda mıknatıslanmıştır.

in the data. Figure 4a-d show the ETHDR images of the synthetic magnetic data in Figure 1a that have been corrupted with random noise of amplitude equal to 1%, 2%, 3% and 5% of the maximum magnetic data amplitude, respectively. The results show that the noise should be smaller in amplitude than the actual edges of sources (e.g., noise levels of %1 and %2). In this case, the edges are clearly resolved. For

relatively high levels of noise, the method will not be able to discriminate between edges and noise (see the response of south-east body in Figure 4d).

APPLICATION TO AEROMAGNETIC DATASET

For comparison, the present and previous methods are demonstrated on an aeromagnetic
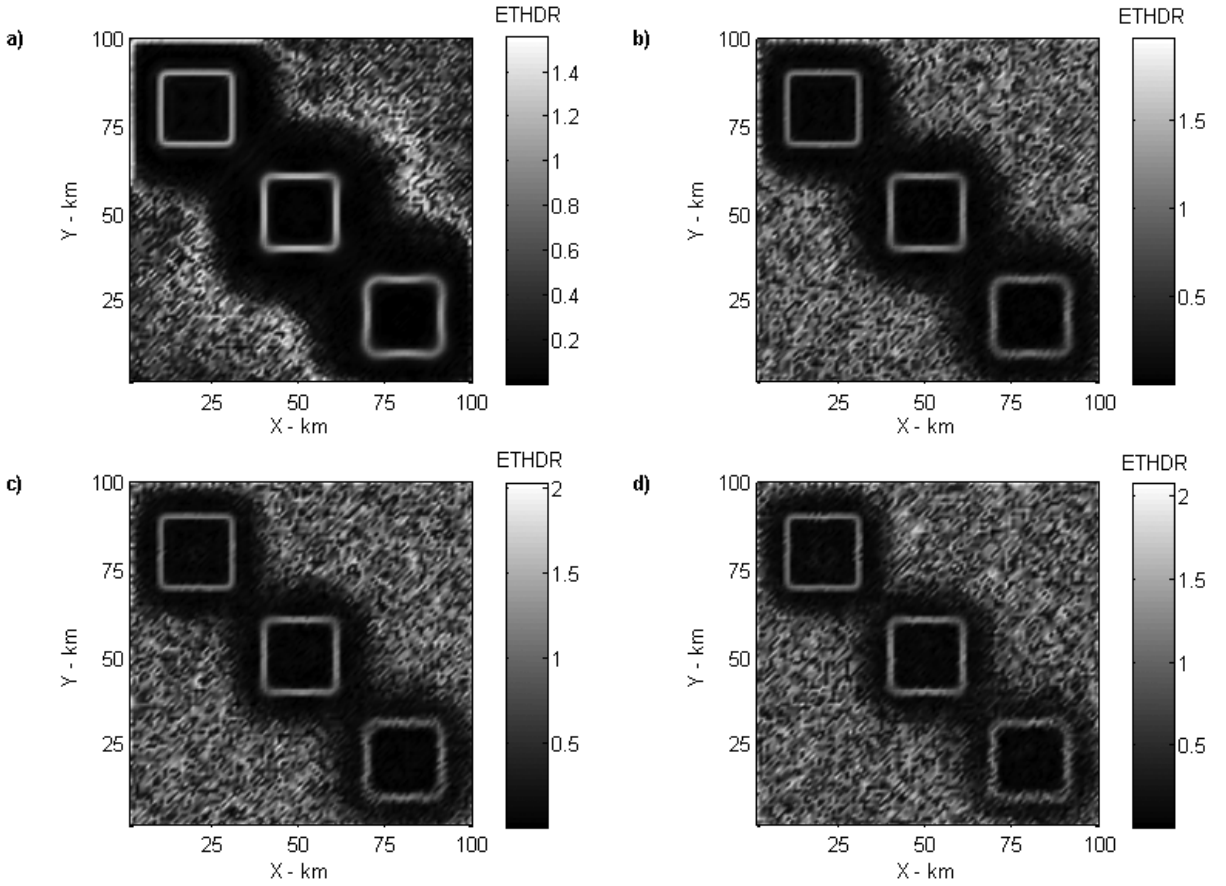
Figure 4. A comparison of different amounts of noise effects on the ETHDR responses. (a) ETHDR image map of magnetic data in Figure 1a. Random noise of amplitude equal to 1% of the maximum magnetic data amplitude is added to the magnetic data. (b) ETHDR image map of magnetic data in Figure 1a. Random noise of amplitude equal to 2% of the maximum magnetic data amplitude is added to the magnetic data. (c) ETHDR image map of magnetic data in Figure1a. Random noise of amplitude equal to 3% of the maximum magnetic data amplitude is added to the magnetic data. (d) ETHDR image map of magnetic data in Figure 1a. Random noise of amplitude equal to 5% of the maximum magnetic data amplitude is added to the magnetic data.

Şekil 4.   Farklı miktarlarda gürültünün ETHDR sonuçları üzerine etkileri. (a) Şekil 1' de verilen manyetik verinin ETH-DR görüntü haritası. Manyetik veriye, manyetik verinin en büyük genlik değerinin 1%' i kadar gelişigüzel rastsal gürültü eklenmiştir. (b Şekil 1' de verilen manyetik verinin ETHDR görüntü haritası. Manyetik veriye, manyetik verinin en büyük genlik değerinin 2%' si kadar gelişigüzel rastsal gürültü eklenmiştir. (c) Şekil 1' de verilen manyetik verinin ETHDR görüntü haritası. Manyetik veriye, manyetik verinin en büyük genlik değerinin 2%' ü kadar gelişigüzel rastsal gürültü eklenmiştir. (d) Şekil 1' de verilen manyetik verinin ETHDR görüntü haritası. Manyetik veriye, manyetik verinin en büyük genlik değerinin 5%' i kadar gelişigüzel rastsal gürültü eklenmiştir.

data from Eskisehir and surrounding region. The tectonic map and the original aeromagnetic data of the Eskisehir and surrounding region is shown in Figure 5a and Figure 5b, respectively. The aeromagnetic data is 170×170 km in size and has a grid resolution of 1 km in both horizontal directions. The data mostly covers the Eskisehir fault zone, which comprises of successive fault segments (Koçyiğit, 2000). The Eskisehir fault and its segments extend in a Northwest to Southeast direction. Figure 5c shows reduction to pole (Baranov, 1957; Baranov and Naudy, 1964) applied aeromagnetic data. Figure 5d is the total horizontal derivative and Figure 5e is the analytical signal of the magnetic data in Figure 5c, respectively. The
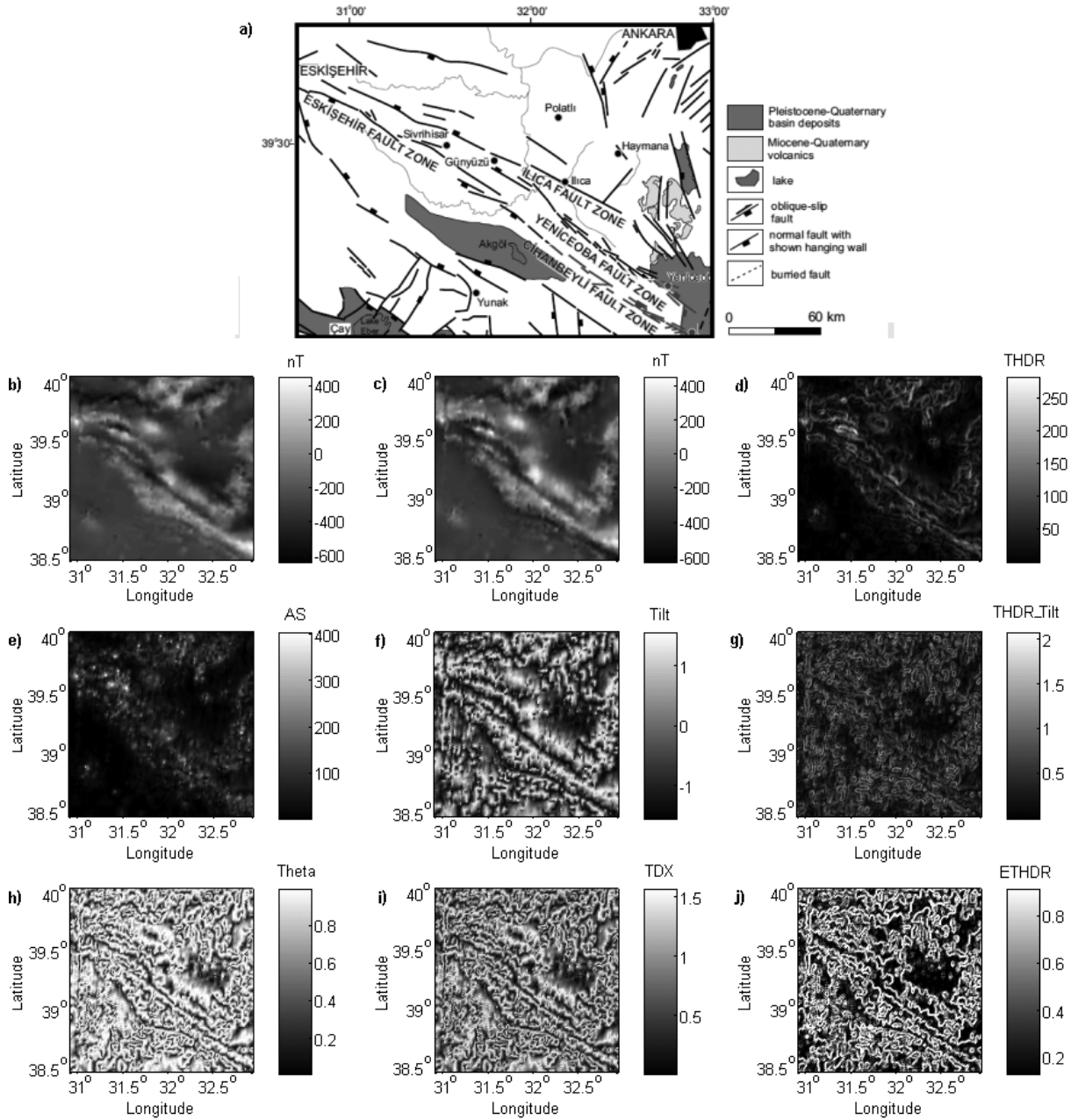
Figure 5. Application to aeromagnetic data: (a) Tectonic map of the Eskisehir and surrounding region (modified from Özsayın and Dirik, 2007). (b) Original aeromagnetic image from the Eskisehir region. Aeromagnetic data covers a 170×170 km area. Grid interval is 1 km in both horizontal directions. (c) Reduced to magnetic pole aeromagnetic image from the Eskisehir region in (b). (d) Total horizontal derivative of magnetic data in (c). (e) Analytical signal of magnetic data in (c). (f) Tilt angle of magnetic data in (c). (g) Total horizontal derivative of the tilt angle (THDR_Tilt) of magnetic data in (c). (h) Theta map of magnetic data in (c). (i) Horizontal tilt angle (TDX) of magnetic data in (c). (j) Enhanced total horizontal derivative of the tilt angle (ETHDR) of magnetic data in (c).

Şekil 5. Havadan manyetik veri üzerinde uygulama: (a) Eskişehir bölgesi ve civarının tektonik haritası (Özsayın ve Dirik, 2007' den değiştirilerek alınmıştır). (b) Eskişehir bölgesi havadan manyetik veri görüntü haritası. Veri 170×170 km' lik bir alanı göstermektedir. Grid aralığı her iki yatay yönde 1 km' dir. (c) (b)' de verilen Eskişehir bölgesi manyetik verisinin kutba indirgenmiş görüntü haritası. (d) (c)' de verilen manyetik verinin toplam yatay türevi. (e) (c)' de verilen manyetik verinin analitik sinyali. (f) (c)' de verilen manyetik verinin eğim açısı. (g) (c)' de verilen manyetik verinin eğim açısı toplam yatay türevi (THDR_Tilt). (h) (c)' de verilen manyetik verinin Theta haritası. (i) (c)' de verilen manyetik verinin yatay eğim açısı (TDX). (j) (c)' de verilen manyetik verinin geliştirilmiş eğim açısı toplam yatay türevi (ETHDR).

original aeromagnetic, reduction to pole applied aeromagnetic, total horizontal derivative and analytical signal images are dominated by the high-amplitude anomalies from Eskisehir fault zone and its segments. Figure 5f-i show the Tilt, THDR_Tilt, theta map and TDX, respectively. Figure 5j shows the ETHDR image of the magnetic data in Figure 5c. The results of the normalized derivative methods in Figure 5f-i show greatly improved detail, particularly in the southwest region. Nevertheless, the results are more diffuse than the ETHDR image in Figure 5j.

CONCLUSIONS and RECOMMENDATIONS

A new edge detection filter, ETHDR, has been introduced for interpretation of magnetic data. The filter has been compared with other commonly used edge detection filters; it gives very sharp response over edges of sources compared with the existing filters. The results show that ETHDR is an effective tool for enhancing subtle detail and delineating edges of shallow and deep structures in magnetic data. The filter was demonstrated using both synthetic and an aeromagnetic dataset. Basically the ETHDR produces an image that is close to pi/2 when the vertical derivative is positive and is close to -pi/2 when vertical derivative is negative. Hence the ETHDR edge detector shows similar behavior as zero contour of vertical derivative. The ETHDR filter strongly amplifies noise in the data as it uses derivatives of a derivative-based filter. Before application of the ETHDR filter on the noisy data, an upward continuation of the magnetic anomaly or low-pass filtering may reduce the noise effect. It is believed that, within the edge enhancement concept, future researchers will introduce many new methods.

REFERENCES

Baranov, V., 1957. A new method for interpretation of aeromagnetic maps, Pseudogravimetric anomalies. Geophysics, 22, 359–383.

Baranov,V., and H. Naudy, 1964. Numerical calculation of the formula of reduction to the magnetic pole. Geophysics, 29, 67–79.

Cooper, G.R.J., 2009. Balancing images of potential-field data. Geophysics, 74(3), L17-L20.

Cooper, G.R.J., and Cowan, D.R., 2006. Enhancing potential field data using filters based on the local phase. Computers & Geosciences, 32(10), 1585-1591.

Cooper, G.R.J., and Cowan, D.R., 2008. Edge enhancement of potential-field data using normalized statistics. Geophysics, 73(3), H1-H4.

Cordell, L., and V.J.S. Grauch, 1985. Mapping basement magnetization zones from aeromagnetic data in the San Juan basin, New Mexico, in W. J. Hinze, ed., The utility of regional gravity and magnetic anomaly maps: SEG, 181-197.

Koçyiğit, A., 2000. Seismicity of the southwestern part of Turkey. BADSEM 2000-Symposium on Seismicity of the Southwestern part of Turkey, İzmir, 30-39.

Li, X., 2006. Understanding 3D analytic signal amplitude. Geophysics, 71(2), B13-B16.

Miller, H.G., and Singh, V., 1994. Potential field tilt—a new concept for location of potential filed sources. Journal of Applied Geophysics, 32, 213-217.

Özsayın, E., and Dirik, K., 2007. Quaternary activity of the Cihanbeyli and Yeniceoba Fault zones: İnönü-Eskişehir fault system, central Anotalia. Turkish Journal of Earth Sciences. 16, 471-492.

Pilkington, M., and Keating, P., 2004. Contact mapping from gridded magnetic data – a comparison of techniques, Exploration Geophysics, 35, 206-311.

Roest, W.R., Verhoef, J., and Pilkington, M., 1992. Magnetic interpretation using the 3-D analytic signal. Geophysics, 57(1), 116-125.

Verduzco, B., Fairhead, J.D., Green, C.M., and MacKenzie, C., 2004. New insights into magnetic derivatives for structural mapping. The Leading Edge, 23(2), 116-119.

Wijns, C., Perez, C., and Kowalczyk, P., 2005. Theta map: edge detection in magnetic data. Geophysics, 70(4), L39-L43.